Dalton Transactions

Accepted Manuscript

Cite this: DOI: 10.1039/c0xx00000x

www.rsc.org/xxxxxx

ARTICLE TYPE

Paramagnetic and Theoretical Study of $Y_2@C_{81}N$: an Endohedral Azafullerene Radical

Zhuxia Zhang,*[a,b] Taishan Wang,*[b] Bingshe Xu,[a] and Chunru Wang*[b]

Received (in XXX, XXX) Xth XXXXXXXXX 20XX, Accepted Xth XXXXXXXXX 20XX
DOI: 10.1039/b000000x

A metallofullerene radical $Y_2@C_{81}N$ was synthesized and characterized by ESR spectroscopy and *ab initio* calculations. It was revealed that the molecule adopts an unique azafullerene $C_{81}N$ cage derived from C_{82}-C_{2v}(9), and two yttrium ions are entrapped to form the endohedral structure. The unpaired electron of $Y_2@C_{81}N$ radical was calculated to mainly localize on the Y_2 dimer, leading to large hyperfine coupling constants of 75.7 and 69.8 G for the two yttrium nuclei, respectively.

Introduction

Endohedral metallofullerene (EMF) radicals have promising applications in quantum information processing and single molecular magnet. However, due to their relative lower stability than those diamagnetic EMF species, most studies so far have focused on the several well-known molecules, e.g., $Sc_3C_2@C_{80}$, $Sc@C_{82}$, $Y@C_{82}$, $La@C_{82}$ and $Gd@C_{82}$, as well as their exohedral derivatives.[1-4]

However, along with the preparation of a new type endohedral azafullerene (EAF) with N-hybridization by introducing nitrogen in the synthetic process, the family of EMF radicals has been largely expanded. Electronic paramagnetic resonance (ESR) study revealed many new features of the EAF radicals. For examples, both $Y_2@C_{79}N$ and $Gd_2@C_{79}N$ are paramagnetic and their unpaired spins localize on the internal M_2 dimer,[5, 6] and theoretical calculations revealed that their spin-containing orbitals are below the highest occupied molecular orbital (HOMO). As comparison, the spin-containing orbital in $La_3N@C_{79}N$ isomer[7, 8] is just the HOMO. Recently, based on the temperature-dependent ESR spectrometry of $Y_2@C_{79}N$, it was revealed a controllable paramagnetism and susceptible internal dynamics in EAF radicals.[9, 10] The EAF species show interesting paramagnetic properties and very promising applications in single molecular magnet, therefore, they have attracted much interest among researchers.

In the isolation process of $Y_2@C_{79}N$, a trace of $Y_2C_{81}N$ was also detected by mass spectrometry as well as ESR spectroscopy. Because the small quantity of $Y_2C_{81}N$ is mixed with an $Y_2@C_{82}$ isomer, it is difficult to separate them completely by the high performance liquid chromatography (HPLC) technique and characterize the geometric structure experimentally. Therefore, *ab initio* calculations were performed to elucidate the possible structure of $Y_2C_{81}N$, and its paramagnetic property was also explored together with the ESR results.

Experimental details

The yttrium EMFs are synthesized by the Krästchmer–Huffman arc discharging method under a mixed atmosphere of He and N_2, and the soot was extracted by toluene solution, and isolated by the HPLC technique with two complementary columns, i.e., Buckyprep and Buckyprep-M. A mixture of $Y_2C_{81}N$ and $Y_2@C_{82}$ was obtained, as characterized by the matrix assisted laser desorption ionization-time of flight (MALDI-TOF) mass spectrometry and ESR spectroscopy.

Computational Details

Optimization of the molecular structures was performed using density functional theory (DFT) implemented in the DMol[3]. The atomic orbitals are represented by a double-numeric quality basis set with polarization functions (DNP), which are comparable to Gaussian 6-31G** sets. The exchange correlation interactions are described by the Perdew−Burke−Ernzerhof generalized gradient approximation (GGA). All atomic positions are fully relaxed at the GGA level without symmetry restriction until the atomic forces are smaller than 10^{-5} Hartree. The electronic structure is obtained by solving the Kohn−Sham equations self-consistently in the spin-polarized scheme, and the self-consistent field procedure is carried out with a convergence criterion of 10^{-6} Hartree on the energy and electron density. The spin-unrestricted algorithm was employed.

For $Y_2C_{81}N$ molecule, it has three possible structures: i.e., $Y_2NC@C_{80}$, $Y_2C_2@C_{79}N$ and $Y_2@C_{81}N$. Gaussian 09 package was employed to optimize the most stable isomer with the hybrid functionals of B3LYP. Y atom was treated by a small-core quasi-relativistic effective core potentials of Dolg et al.[11, 12] together with the optimized basis set for the valence shells with a contraction scheme of (8s7p6d2f1g)/ [6s5p3d2f1g].

In computations of hyperfine coupling constant (hfcc) with the

ORCA package[13], we used the PBE functional and def2-TZVP basis sets.

Results and discussions

Due to the low yield of $Y_2C_{81}N$ in toluene solution, it was difficult to isolate it from $Y_2@C_{82}$. As shown in Fig. 1a, only a trace of this molecule was observed from the abnormal isomeric distributions of $Y_2@C_{82}$ in the mass spectrum, where the emerging peak of m/z = 1164 implied a new molecule of $Y_2C_{81}N$. Since the high sensitivity of ESR spectrometry and the fact that $Y_2@C_{82}$ is known as diamagnetic species, the existence of $Y_2C_{81}N$ was naturally concluded from the following ESR study. Fig. 1b exhibits the experimental ESR spectrum measured at 298 K, which is obviously different with any other known paramagnetic Y_nC_m or $Y_nC_mN_q$ isomers.

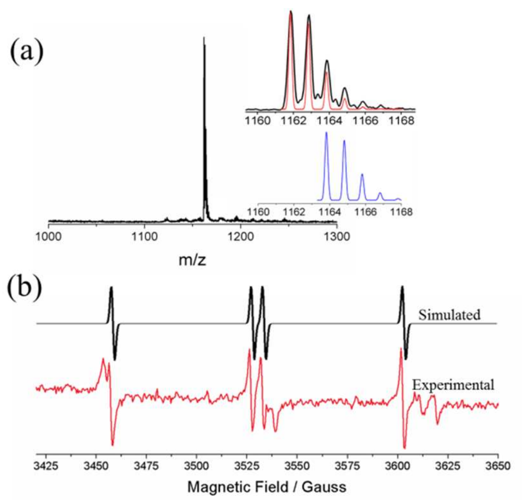

Fig. 1 (a) The MALDI-TOF mass spectrum of $Y_2@C_{82}$ and $Y_2C_{81}N$ mixture. The insets show the isotopic distributions of experimental peak (black line), simulated peak of Y_2C_{82} (red line), and simulated peak of $Y_2C_{81}N$ (blue line). (b) The ESR spectrum of $Y_2@C_{82}$ and $Y_2C_{81}N$ mixture measured in CS_2 at 298 K. The simulated ESR spectrum of $Y_2@C_{81}N$ was illustrated as well.

Detailed analysis of the ESR spectrometry of $Y_2C_{81}N$ revealed two hfcc parameters of 75.7 and 69.8 G for the two Y nuclei and a g-value of 1.97851. For mono-metallofullerenes, such as $Sc@C_{82}$ and $Y@C_{82}$, their unpaired spin locates on the carbon cage and this type of spin distributions results in small hfcc (3.82 for $Sc@C_{82}$； 035 for $Y@C_{82}$)[14]. However in other paramagnetic metallofullerenes species, their metal nuclei bear the unpaired spin and bring about large hfcc. For example, $Y_2@C_{82}$-C_s anion radical has hfcc at 34.3 G (two nuclei),[10] $Sc_3N@C_{80}$ anion radical has hfcc at 55.7 G (three nuclei),[15] $Y_2@C_{79}N$ molecule has hfcc at 81.2 G (two nuclei), and $Sc_4O_2@C_{80}$ cation radical has hfcc at 150.4 G,[16] etc. In all of the above mentioned metallofullerenes the spin was found to be localized on internal metal nuclei. That is because that the size of the isotropic hfcc is mainly determined by the ns-orbital contributions to the spin density: the large contribution of ns-orbitals to the SOMO (and therefore a spin density) leads to the large value of the coupling constant.[17] Therefore, the large hfcc values of $Y_2C_{81}N$ suggests that the unpaired spin would mainly reside on the two Y_2 nuclei, which provides a valuable clue for the following structural assignments by theoretical calculations.

Three possible structures of $Y_2C_{81}N$, i.e., $Y_2CN@C_{80}$, $Y_2C_2@C_{79}N$ and $Y_2@C_{81}N$ were calculated. Comparing studies on $Y_2C_2@C_{80}$ anion, $Y_2C_2@C_{79}N$, and $Y_2CN@C_{80}$ were performed and their calculated spin distributions are shown in Fig. S2. Obviously, in all of the optimized structures based on C_{80} and $C_{79}N$, the unpaired spins are localized on fullerene cages but not the yttrium nuclei, that is inconsistent with the experimental ESR measurements, and hence the two structures can be ruled out and the only possible candidate of $Y_2C_{81}N$ is in the form of $Y_2@C_{81}N$.

$Y_2@C_{82}$ was one of the first isolated Y-based EMFs, and the structure of its main isomer is known to be based on the $C_{3v}(8)$ cage.[18] The carbon cage of $Y_2@C_{82}$-$C_{3v}(8)$ corresponds to that of most stable isomer of empty C_{82} in the 4- charge state. In 2005, Hino et al. reported an ultraviolet photoelectron spectra (UPS) study of $Y_2@C_{82}$-$C_{3v}(8)$ where they supposed that the Y adopts trivalent state.[19] While DFT calculations for the same molecule by Popov et al. showed that the divalent state of Y is more appropriate.[18] As pointed by Popov *et al.* based on their MO analysis, the M-M bonding orbitals in $Y_2@C_{82}$-$C_{3v}(8)$ are predicted as the HOMO, which can be transformed into SOMOs by one-electron transfer to/from the molecule.[17] Considering the large hfcc (75.7 and 69.8G) of $Y_2C_{81}N$ in ESR experimental result, therefore, the $Y_2@C_{81}N$ derived from C_{82}-$C_{3v}(8)$ was investigated firstly.

C_{82}-$C_{3v}(8)$ cage has 17 kinds of different carbon atoms, leading to 17 $C_{81}N$ isomers after substituting carbon atom with N atom at different sites. Since in most cases the internal species in endohedral fullerenes show dynamic motion inside the fullerene cages, e.g., in $Sm@C_{74}$-D_{3h}, the Sm atom is highly disordered reflecting a motional Sm atom inside cage.[20] In addition, the Sc_2C_2 cluster rotates freely in C_{84}.[21] Herein, for $Y_2@C_{81}N$ structure, Y-Y dimer was considered to set on 7 different orientations for each $C_{81}N$ isomer, and finally 119 isomers of $Y_2@C_{81}N$ were screened by GGA-PBE/DNP in Dmol[3] software (see Fig. S3).

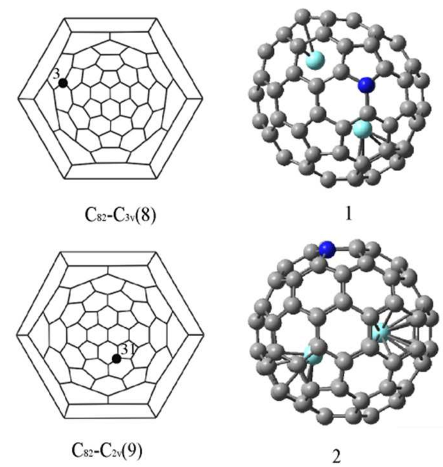

Fig. 2 Schlegel diagrams for C_{82}-$C_{3v}(8)$ and C_{82}-$C_{2v}(9)$. B3LYP-optimized molecular structures: (1) the most stable $Y_2@C_{81}N$-$C_{3v}(8)$; (2). $Y_2@C_{81}N$-$C_{2v}(9)$ C, N and Y atoms are shown as gray, blue and green spheres. In Isomer 2, Y_2 dimer is along the belt of 10 continuous hexagons.

Fig. 2 shows the most stable structure (Isomer 1) for

$Y_2@C_{81}N$-$C_{3v}(8)$, in which the N atom replaces a carbon atom denoted as C3 at the hexagon/hexagon/pentagon junction (665 junction). Previous computational studies also indicated that the 665 junctions are the preferred sites for N atom in the $Y_2@C_{79}N$[6] and $Sc_3N@C_{79}N$.[22] Moreover, it was revealed that the encapsulated Y-Y dimer stays near the carbon walls rather than at the center of cage, and the Y atoms tend to far away from the N atom. Fascinatingly, the Y-N-Y tends to form a triangle shape with the N atom always locating above the Y-Y bonds.

In Isomer 1, as listed in Table 1, the distances between Y and the nearest C atoms is 2.36Å, and the distance of Y-Y is 4.24 Å which is longer than that in $Y_2@C_{82}$-$C_{3v}(8)$ (3.695 Å) and $Y_2@C_{79}N$(3.934 Å) [17]. That is because, for $Y_2@C_{82}$-$C_{3v}(8)$, the HOMO is localized on Y-Y dimer with two 5s-electrons filled in, but when the N atom being involved in $Y_2@C_{81}N$, one 5s-electron in the HOMO becomes the spin electron with a bond order of 0.5 for the Y–Y bonding orbitals, resulting in an elongated Y-Y distance. Moreover, the calculated HOMO-LUMO gap of $Y_2@C_{81}N$-$C_{3v}(8)$ is 1.10 eV in B3LYP level, which is larger than 0.26 eV of $Y_2@C_{82}$-$C_{3v}(8)$[17], suggesting a stable structure of $Y_2@C_{81}N$. The α-spin and β-spin orbital levels for the open-shell $Y_2@C_{81}N$ are separately listed in Table 1. As shown in Fig. 3a, the unparalleled spin orbital locates at a much lower energy level than the HOMO, hence the Aufbau principle is violated in this case. For α-orbital in Isomer 1, the spin orbital derives from HOMO-2~5, which is composed of the hybridized 4p5s orbitals of Y and a few π orbitals of $C_{81}N$. Similar behavior was also observed in corresponding beta orbital (shown in Fig. S4). Its LUMO-1 is composed of the 5s-orbital of Y nuclei. Detailed analyses of its Kohn-Sham molecular orbtials reveal that $Y_2@C_{81}N$-$C_{3v}(8)$ has an electronic structure of $[Y_2]^{5+}@[C_{81}N]^{5-}$.

Table 1 The relative energy (RE, kcal/mol), distance between Y and the nearest C atom ($d_{Y–C}$, Å), Y-Y distance($d_{Y–Y}$, Å), HOMO–LUMO gap (eV) Mulliken spin densities of Y ($Spin_Y$) and hyperfine coupling constants (a, Gauss) calculated by DFT method

Isomer	RE	$d_{Y–C}$	$d_{Y–Y}$	HOMO	LUMO	Gap	Spin(Y)	a
1	0	Y1: 2.36 Y2: 2.36	4.24	α -4.65 β -4.64	α -3.53 β –3.54	α 1.12 β 1.10	Y1: 0.325 Y2: 0.503	Y1: 47.29 Y2: 56.18
2	10.39	Y1: 2.34 Y2: 2.42	3.96	α -4.91 β -4.91	α -3.09 β -3.35	α 1.82 β 1.56	Y1: 0.500 Y2: 0.482	Y1: 61.86 Y2: 62.26

[a] [a] The α-spin and β-spin orbital levels for the open-shell $Y_2@C_{81}N$ are individually listed in Table 1.

Noting that $[C_{81}N]^{5-}$ is isoelectronic with $[C_{82}]^{6-}$, and among all known isomers C_{82}, C_{82}-$C_{2v}(9)$ is the lowest energy isomer of C_{82}^{6-} form,[17] So in this work the geometry optimizations on the $Y_2@C_{81}N$-$C_{2v}(9)$ were also considered at B3LYP level. Isomer 2 is the most stable $Y_2@C_{81}N$-$C_{2v}(9)$ structure, in which the N atom replaces C31 atom (shown in Fig.2). Parts of the structural and electronic parameters of Isomer 2 are listed in Table 1.

Isomer 2 is more stable than Isomer 1 by 10.39 kcal/mol. Its HOMO−LUMO gap is larger than that of Isomer 1. The gap and relative energy value is already sufficiently large to conclude that Isomer 2 is thermodynamically and kinetically favorable one.

In Isomer 2, as shown in Fig. 2, the Y_2 dimer is set along the belt of 10 continuous hexagons with one Y atom coordinating with an adjacent hexagon of the cage in η^6-fashion, and the other Y atom locating above the C atom at 665 junction. The computed Y-Y distance for Isomer 2 is 3.96 Å that is shorter than 4.24 Å for Isomer 1. In addition, the corresponding Y-C distances in Isomer 2 are longer than those in Isomer 1, revealing weak interaction between Y_2 dimer and $C_{81}N^-$-$C_{3v}(8)$ cage.

Isomer 2 has similar spin distribution with that in Isomer 1 except for locating on a more narrow energy range (HOMO -4~5). The HOMOs are mainly composed of the 2pπ orbitals of $C_{81}N$ cage, and SOMO orbital locates below the HOMOs and the LUMO is localized between the yttrium ions, so the electronic structure of Isomer 2 can also be represented as $[Y_2]^{5+}@[C_{81}N]^{5-}$.

The net Mulliken spin populations of Y atom were calculated, which are 0.32 and 0.50 for two Y atoms in Isomer 1, and the net spin populations of the Y in Isomer 2 are more uniform (0.50, 0.48). As the 5s-electrons have involved in the spin population that directly affects the couplings of Y nuclei, the hfcc of Y nuclei are expected to be large.

In order to further study the ESR property of $Y_2@C_{81}N$ and determine its structure, we calculated the hfcc of two $Y_2@C_{81}N$ isomers using ORCA software. The calculated large hfcc values for Isomer 1 and 2 are listed in Table 1. While the calculated hfcc (61.86 and 62.26 G) for Isomer 2 are more close to the experimental ESR results (75.7 and 69.8 G). So we further confirm that the isolated isomer in our experiment is $Y_2@C_{81}N$-$C_{2v}(9)$.

Conclusions

The $Y_2C_{81}N$ endohedral fullerene radical was detected by the MALDI-TOF mass spectrometry and ESR spectroscopy. The calculated structure has been assigned as $Y_2@C_{81}N$-$C_{2v}(9)$ with a formal transfer of five electrons from the Y_2 cluster to the cage. DFT calculation indicates that in optimized $Y_2@C_{81}N$ the unpaired spin electron resides on the internal Y_2 dimer, which is consistent with the experimental ESR result. These studies on $Y_2@C_{81}N$ expand the family of endohedral azafullerenes, which have many interesting properties in quantum information progressing and molecular magnet.

We thank the National Basic Research Program (2012CB932900), the National Natural Science Foundation of China (21203205, 51002102, 21121063), and NSAF (11179006).

Notes and references

[a] *Key Laboratory of Interface Science and Engineering in Advanced Materials, Taiyuan University of Technology, Ministry of Education, Research Center of Advanced Materials Science and Technology, Taiyuan University of Technology, Taiyuan 030024, China. Fax:86-351-6010311; Tel: 86-351-6010384; E-mail: zhangzhuxia@tyut.edu.cn.*

[b] *Beijing National Laboratory for Molecular Sciences, Laboratory of Molecular Nanostructure and Nanotechnology, Institute of Chemistry, Chinese Academy of Sciences, Beijing 100190, China. Fax: 86-10-62652120; Tel: 86-10-62652120; E-mail: wangtais@iccas.ac.cn, crwang@iccas.ac.cn.*

† Electronic Supplementary Information (ESI) available: [details of any supplementary information available should be included here]. See DOI: 10.1039/b000000x/

‡ Footnotes should appear here. These might include comments relevant to but not central to the matter under discussion, limited experimental and spectral data, and crystallographic data.

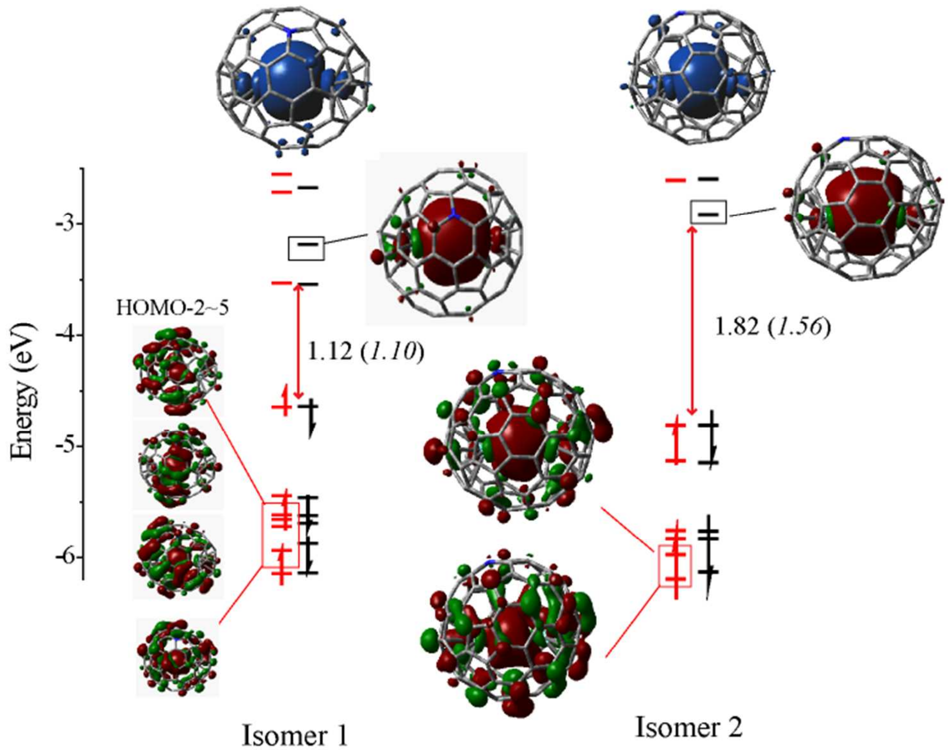

Fig. 3 The calculated spin density distributions and Kohn-Sham molecular orbitals for Isomer 1 and 2, (normal font for α-spin, and italic font for β-spin). The blue area presents the unpaired spin, which is shown upper part of the figure and orbital energies are shown at the lower part along with drawings of the critical yttrium-based orbitals that contain the free spin.

1. M. Yamada, T. Akasaka and S. Nagase, *Accounts of chemical research*, 2010, **43**, 92-102.
2. X. Lu, T. Akasaka and S. Nagase, *Chem Commun (Camb)*, 2011, **47**, 5942-5957.
3. A. A. Popov and L. Dunsch, *The Journal of Physical Chemistry Letters*, 2011, **2**, 786-794.
4. B. J. Farrington, M. Jevric, G. A. Rance, A. Ardavan, A. N. Khlobystov, G. A. D. Briggs and K. Porfyrakis, *Angewandte Chemie International Edition*, 2012, **51**, 3587-3590.
5. S. Nagase, K. Kobayashi and T. Akasaka, *Journal of Molecular Structure: THEOCHEM*, 1999, **461–462**, 97-104.
6. T. Zuo, L. Xu, C. M. Beavers, M. M. Olmstead, W. Fu, T. D. Crawford, A. L. Balch and H. C. Dorn, *Journal of the American Chemical Society*, 2008, **130**, 12992-12997.
7. S. Stevenson, Y. Ling, C. E. Coumbe, M. A. Mackey, B. S. Confait, J. P. Phillips, H. C. Dorn and Y. Zhang, *Journal of the American Chemical Society*, 2009, **131**, 17780-17782.
8. X. Lu, L. Feng, T. Akasaka and S. Nagase, *Chemical Society reviews*, 2012, **41**, 7723-7760.
9. Y. Ma, T. Wang, J. Wu, Y. Feng, L. Jiang, C. Shu and C. Wang, *Chem Commun (Camb)*, 2012, **48**, 11570-11572.
10. Y. Ma, T. Wang, J. Wu, Y. Feng, H. Li, L. Jiang, C. Shu and C. Wang, *The Journal of Physical Chemistry Letters*, 2013, **4**, 464-467.
11. J. M. L. Martin and A. Sundermann, *The Journal of Chemical Physics*, 2001, **114**, 3408.
12. D. Andrae, U. Häußermann, M. Dolg, H. Stoll and H. Preuß, *Theoret. Chim. Acta*, 1990, **77**, 123-141.
13. F. Neese, *Wiley Interdisciplinary Reviews: Computational Molecular Science*, 2012, **2**, 73-78.
14. A. A. Popov, S. Yang and L. Dunsch, *Chemical reviews*, 2013, **113**, 5989-6113.

15. A. A. Popov and L. Dunsch, *Journal of the American Chemical Society*, 2008, **130**, 17726-17742.
16. A. A. Popov, N. Chen, J. R. Pinzon, S. Stevenson, L. A. Echegoyen and L. Dunsch, *Journal of the American Chemical Society*, 2012, **134**, 19607-19618.
17. A. A. Popov, S. M. Avdoshenko, A. M. Pendas and L. Dunsch, *Chem Commun (Camb)*, 2012, **48**, 8031-8050.
18. A. A. Popov and L. Dunsch, *Chemistry*, 2009, **15**, 9707-9729.
19. S. Hino, N. Wanita, K. Iwasaki, D. Yoshimura, T. Akachi, T. Inoue, Y. Ito, T. Sugai and H. Shinohara, *Physical Review B*, 2005, **72**.
20. W. Xu, Y. Hao, F. Uhlik, Z. Shi, Z. Slanina and L. Feng, *Nanoscale*, 2013.
21. H. Kurihara, X. Lu, Y. Iiduka, H. Nikawa, M. Hachiya, N. Mizorogi, Z. Slanina, T. Tsuchiya, S. Nagase and T. Akasaka, *Inorganic chemistry*, 2012, **51**, 746-750.
22. J. Q. Hou and H. S. Kang, *Chemical Physics*, 2007, **334**, 29-35.

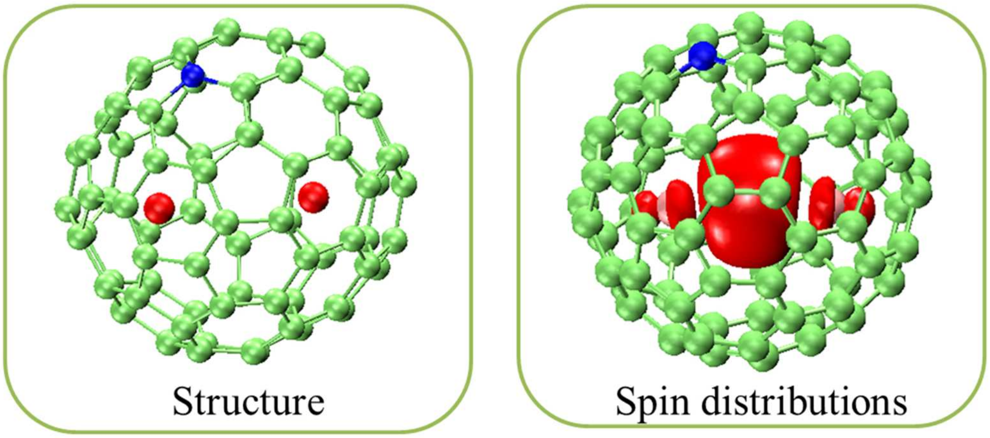

Azametallofullerene of $Y_2@C_{81}N\text{-}C_{2v}(9)$